

Synthesis of a Fully Biobased Polyfunctional Vinyl Oligomer and Their UV Cured Films Prepared via Thiol-ene Coupling

Changqing Fu^{1,2}, Jiahui Wang^{1,2}, Lie Chen^{1,2} and Liang Shen^{1,2,*}

¹Department of Polymer and Coating, Jiangxi Science & Technology Normal University, Nanchang, China.

²Jiangxi Engineering Laboratory of Waterborne Coating, Nanchang, China.

*Corresponding Author: Liang Shen. Email: liangshen@vip.163.com.

Abstract: In this paper, a fully bio-based vinyl oligomer with high functionalities was successfully prepared from rapeseed oil by three modification steps: epoxidation of rapeseed oil, solvent-free and catalyst-free ring opening by 10-undecylenic acid followed by esterification with 10-undecenoyl chloride. Then, the renewable polymers were prepared by photo-polymerization of these modified vegetable oils with typical thiol monomers: pentaerythritol tetrakis (3-mercaptopropionate), pentaerythritol tris (3-mercaptopropionate) and 1,2-ethanedithiol. The synthesis of the vinyl oligomer was monitored by nuclear magnetic resonance and Fourier-transform infrared spectroscopy. The average number of the carbon-carbon double bonds of the resulting vinyl oligomer is high to be 7.2. The kinetic of thiol-ene photo-polymerization of vegetable oil-based vinyl oligomer was studied by FTIR-ATR analyses. In addition, the thermo-physical properties, thermal stability and solvent resistance of these UV cured films were characterized. The polymers from 1,2-ethanedithiol exhibit higher gel content, storage modulus and glass transition temperature than those from other thiol monomers due to the high crosslinking densities of the resulting polymers. All polymers show excellent thermal stability up to 290°C. The resulting polymers exhibit thermo-physical properties, excellent water resistance and thermals stability, which is promising to find application in coatings and adhesives.

Keywords: Vegetable oil; photo-polymerization; thermo-physical properties; thermal stability

1 Introduction

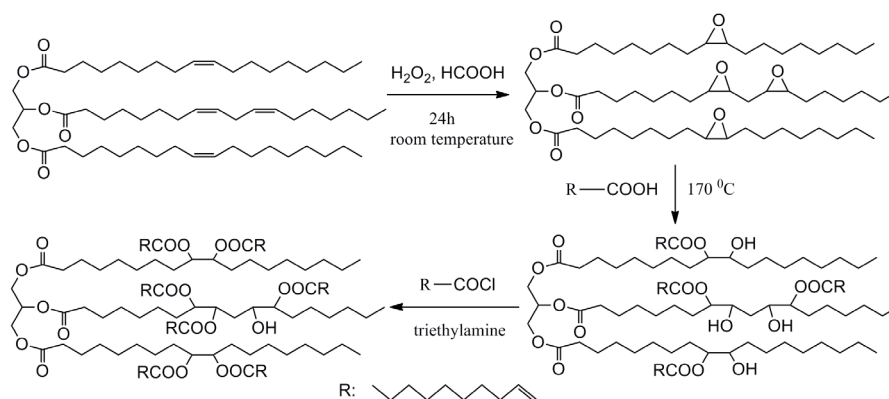
With the depletion of fossil resources and the increasing concerns toward environmental issue, much effort has been dedicated to develop polymeric materials from renewable resource as a replacement of petroleum based counterparts for a sustainable and environment-friendly society [1-4]. Vegetable oils, a typical renewable source, have attracted much attention for this purpose due to their unique properties, such as, ready availability, inherent biodegradability and low toxicity [5-7]. Vegetable oils are tri-esters formed by glycerol and fatty acids containing 8-18 carbon atoms that can be either poly-, mono-, or unsaturated. It is well known that the unsaturated groups of most vegetable oils are located in the middle of fatty acid chains, which show low reactivity for efficient polymerization [8,9]. In addition, the unsaturated degree of vegetable oils is limited, leading to the poor mechanical properties and thermal stability of the resulting polymers. Therefore, the exploit of efficient chemical modification and suitable polymerization method are necessary for development of high performance polymers from vegetable oils, which would widen the application of vegetable oils as a renewable platform chemical [5,8,10-14].

During the last decade, there are many researches focusing on the development of green method for

synthesis of acrylated vegetable oils and their photo-polymerization [14-17]. For example, Kessler et. al. have prepared acrylated soybean oil by epoxidation followed by ring opening with acrylic acid [18]. The homo-polymerization of acrylated soybean oil and copolymerization of acrylated soybean oil [19] and methacrylated vanillin leads to a series of novel, bio-renewable polymers ranging from rigid plastics and soft elastomers [20]. Zhang et al. developed a novel efficient one-step method for preparation of acrylated soybean oil (ASO) directly from soybean oil and acrylic acid under the catalysis of $\text{BF}_3 \cdot \text{Et}_2\text{O}$ [3]. Highly crosslinked rigid polymers have been prepared by copolymerization of the ASO and styrene [21]. However, the environmental factors, such as oxygen or humidity, greatly affect the homo-polymerization of acrylate vegetable oils and their properties, leading to the difficulty in practical application.

Thiol-ene click reaction is a novel reaction with many remarkable advantages, such as rapid polymerization rates, high efficiency and easily accessible [22-26]. Most important of all, it can proceed under mild conditions, which could avoid the above disadvantages of traditional photo-polymerization of acrylate monomers [13,17,27-29].

In this paper, highly branched vegetable oil derivatives with varying degrees of unsaturated double-bonds were successfully prepared by three steps: epoxidation of rapeseed oil, solvent-free and catalyst-free ring opening by 10-undecylenic acid, and esterification with 10-undecenoyl chloride. Then, the renewable polymers were prepared by photo-polymerization of these modified vegetable oils and typical thiol monomers (pentaerythritol tetrakis (3-mercaptopropionate) (PETMP), pentaerythritol tris (3-mercaptopropionate) (PTMP) and 1, 2-ethanedithiol (EDT)). The kinetic of thiol-ene photopolymerization was studied by FTIR-ATR analyses. In addition, the thermos-physical properties and thermal stability of UV-curable films were characterized.



Scheme 1. Synthesis of fully bio-based oligomer

2 Experimental

2.1 Materials

PETMP, PTMP and EDT were purchased from Aldrich China. Rapeseed oil (RO) was purchased from local supermarket. Hydrogen peroxide (30%), 10-undecylenic acid, N, N-dimethylformamide, triethylamine was purchased from Aladdin China. Formic acid, sodium carbonate, sodium hydroxide, anhydrous magnesium sulfate, ethyl acetate and dichloromethane were purchased from Beijing Chemical works. 2-Hydroxy-2-methylpropiophenone (UV1173) was obtained from JiuRi Chemical of China. All materials were used as received without further purification. 10-Undecenoyl chloride was prepared with the method previous reported [30].

2.2 Synthesis of Epoxidized Rapeseed Oil (ERO)

Scheme 1 shows the synthesis route of epoxidized rapeseed oil. Rapeseed oil (5 g, 0.005 mol),

formic acid (5.36 g, 0.117 mol) and 30% hydrogen peroxide (12 g, 0.106 mol) were added to a 100 mL flask equipped with a reflux condenser under vigorous stirring. The reaction was carried out at a constant temperature of 20°C for 24 h. Then, 15 mL ethyl acetate and 10 mL water were added. After the mixture was stirred for a few minutes, the organic layer was washed with aqueous sodium carbonate solution until a slightly alkaline pH was obtained. After that, the ethyl acetate phase was dried over anhydrous magnesium sulfate to remove the trace amounts of water and then filtered. Finally, the clear viscous ERO with 88% yield was obtained after removal of the organic solvent under vacuum.

2.3 Synthesis of The Rapeseed Oil Based Branched Polyols (UROP)

The rapeseed oil polyols were prepared by ring-opening reaction between ERO with 10-undecylenic acid with a solvent-free and catalyst-free method. Briefly, ERO (2 g, 0.002 mol) and 10-undecylenic acid (1.47 g, 0.008 mol) were mixed in a flask equipped with a reflux condenser and a magnetic stirrer, then the ring opening reaction was carried out at 170°C for 8 h. The rapeseed oil-based polyols were obtained with 100% yield.

2.4 Synthesis of the 10-Undecenoyl Modified Rapeseed Oil-based Oligomer (UROO)

The rapeseed oil-based polyols (3.47 g, 0.002 mol) and triethylamine (1.6 g, 0.016 mol) were dissolved in ethyl acetate in a flask equipped with a magnetic stirrer and cooled in an ice bath, and then 10-undecenoyl chloride (3.2 g, 0.016 mol) was added dropwise. After the addition of 10-undecenoyl chloride, the reaction was carried out at ice bath for 2 h and at room temperature for another 24 h. Subsequently, the solution was filtrated and the organic phase was washed several times with 1% sodium hydroxide solution and distilled water, respectively. Finally, the red-brown liquid of UROO was obtained with 85% yield after dry with anhydrous magnesium sulfate and removal of the solvent was removed.

2.5 Preparation of Thiol-eneUV Cured Coatings

The thiol-ene UV curable films were prepared according to the formulations summarized in Tab. 1. The mixtures were homogenized and coated on PTFE panels. A uniform thickness (~60 μm) of the films was obtained by means of a wire-wound drawdown rod. The films were cured under the irradiation of a UV lamp (1700 μW/cm², 365 nm) in air with 10 minutes.

Table 1: Thiol-ene UV cured films codes and compositions

	Oligomer	Thiol (functionality)	C=C/SH	UROO (g)	Thiol (g)	UV 1173 (g)
CF1	UROO	EDT (2)	1:1	1.00	0.15	0.023
CF2	UROO	PTMP (3)	1:1	1.00	0.42	0.028
CF3	UROO	PETMP (4)	1:1	1.00	0.39	0.028

2.6 Characterization

The kinetics of the photo-polymerization was determined by a Bruker-Vertex 70 spectrometer with the attenuated total reflection (ATR) accessory. A drop of deployed coating formulation was placed on total reflection lens and cured on the UV light irradiation (1700 μW/cm², 365 nm), then the IR spectra were collected every 2 minutes during the course of polymerization. The polymerization rate was calculated by measuring the peak area of characteristic peaks. Ene monomer conversion was monitored at the -CH=CH₂ stretching peak around 3078 cm⁻¹ and thiol monomer conversion was monitored at the S-H stretching peak around 2570 cm⁻¹. Conversion of the reactive groups could be calculated by measuring the peak area at each reaction time and determined as $\chi_{(t)} = [(A_0 - A_t) / A_0] \times 100\%$, where $\chi_{(t)}$ is the conversion

of the reactive groups at time t , A_0 is the absorption peak area before UV exposure while A_t is the absorption peak area of the reactive groups at time t .

The chemical structures of the monomers were characterized by ^1H and ^{13}C NMR spectra using a Bruker AV-400 NMR. Tetramethylsilane and deuterated chloroform were used as an internal reference, and solvent, respectively. The thermal stability of the polymers was characterized by thermogravimetric analysis (TGA) using a TGA-Q50 system (TA Instruments) with a heating rate of $10\text{ }^\circ\text{C min}^{-1}$ in a nitrogen atmosphere. The hardness of the polymer films was characterized using a pendulum hardness tester (Sheen Instrument Ltd., UK) according to ASTM D4366.

Gel content of the polymer films was determined by the following procedure: firstly, immerse cured film with a known mass in methylene chloride at room temperature for a pre-determined time, followed by filtering, drying, and reweighing of the solid remnants. Similarly, water absorption measurement was performed at room temperature: firstly, immerse of the dried films ($20\text{ mm} \times 20\text{ mm}$) with a known weight (W_1) in water for a pre-determined time. After the residual water was removed, the weight (W_2) of the wet film was immediately measured. Water absorption of the cured films was calculated using the following equation: $A (\%) = [(W_2 - W_1) / W_1] \times 100$.

With a similar method as reported previously [30], toluene swollen measurement was performed by immersing cured film in a toluene bath. The towel-dried sample weight (W_t) and the oven-dried sample weight (W_0) was obtained after immersion for a pre-determined time. The following equation was used to calculate toluene swollen of the films: $Q (\%) = [(W_t - W_0) / W_0] \times 100$.

3 Results and Discussion

3.1 Synthesis and Characterization of UROO

UROO was synthesized by three steps: epoxidation of RO, solvent-free and catalyst-free ring opening by 10-undecylenic acid, and esterification with 10-undecenoyl chloride.

Fig. 1 shows the ^1H NMR spectra of RO, ERO, UROP and UROO. The peaks at 5.35 ppm and 2.0 ppm corresponding to $\text{CH}=\text{CH}-$ of RO disappear in the spectra of the ERO and newly peaks corresponding to epoxy groups appear from 2.8 ppm to 3.2 ppm, indicating the successful epoxidation of RO. The disappearance of epoxy groups at 2.8-3.2 ppm, and the newly appearance of peaks corresponding to hydroxyl groups at 3.5-3.7 ppm and $-\text{CH}=\text{CH}_2$ at 4.8-5.1 ppm in the spectra of UROP indicate the completely ring opening of ERO with 10-undecylenic acid as expected. After react with 10-undecenoyl chloride, the hydroxyl groups completely consumed as evidenced by the disappearance of hydroxyl groups at 3.5-3.7 ppm and more $-\text{CH}=\text{CH}_2$ groups are successfully grafted at the backbone of triglyceride as evidenced by the enhancement of 4.8-5.1 ppm spectra, leading to the formation of UROO. According to the ^1H NMR spectra of UROO, the number of terminal carbon-carbon double bonds per triglyceride of UROO was determined by the ratios of the peak area of the signal located at 5.8 ppm based on the normalization of the methyl proton peak areas located at 0.88 ppm. The average number of the carbon-carbon double bonds of UROO is found to be 7.2.

The chemical structure of the resulting UROO was also verified by ^{13}C NMR as shown in Fig. 2. The signals in the range of 127-132 ppm of RO are associated with the double bonds of triglycerides, which disappear in the ^{13}C NMR of ERO because of the epoxidation of double bonds. In addition, the signals corresponding to carbons of newly formed epoxy groups at 54 ppm and 57 ppm are observed in the spectra of ERO. There is no big difference between the ^{13}C NMR spectra of UROP and that of UROO. The chemical shifts of 172.1 and 166.5 ppm of UROO are attributed to the carbonyls of triglyceride and carbonyls of ester, respectively. The chemical shifts associated with the double bonds of 10-undecylenic acid appear at 137 and 112.5 ppm.

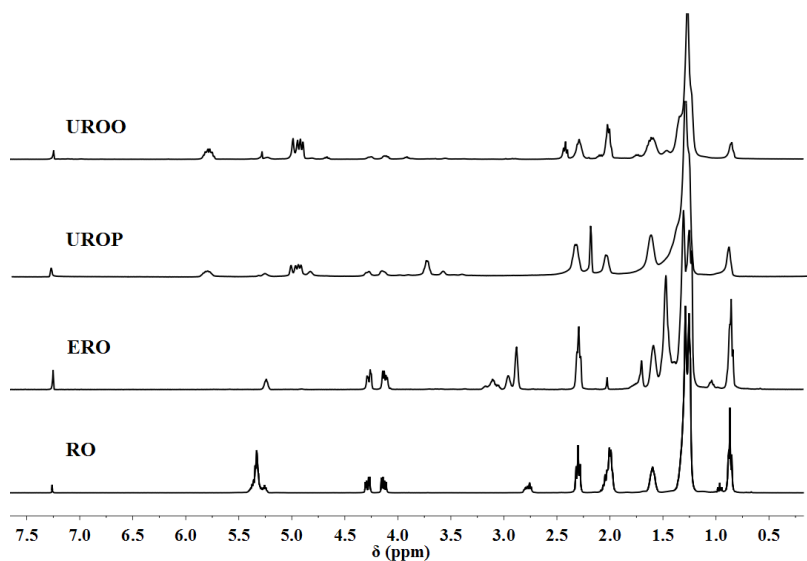


Figure 1: ^1H NMR spectra of RO, ERO, UROP and UROO

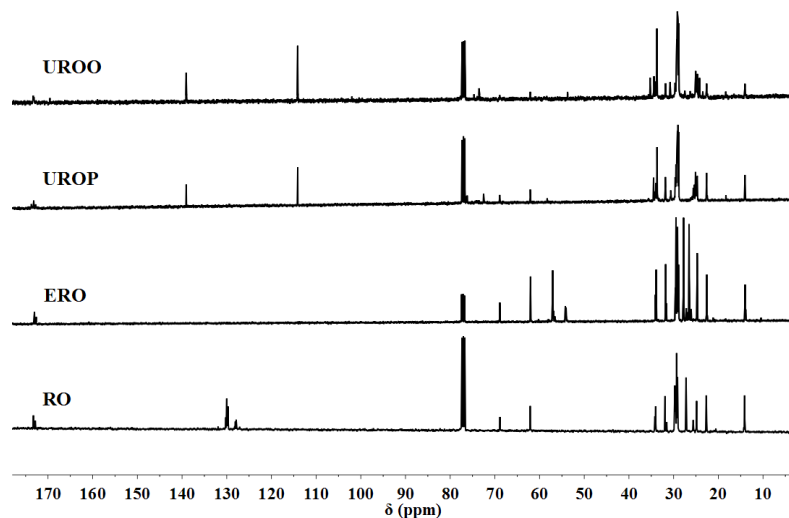


Figure 2: ^{13}C NMR spectra of RO, ERO, UROP and UROO

The transformation of rapeseed oil to bio-based vinyl oligomer, UROO, was also monitored by FTIR as shown in Fig. 3. The signals of carbon-carbon double bond at 3008 cm^{-1} and 1643 cm^{-1} which are present in the spectra of RO, disappear in the spectra of ERO. Meanwhile, the signals of epoxy groups at 910 cm^{-1} and 801 cm^{-1} are present in the spectra of ERO. Two new peaks corresponding to terminated double bonds of 10-undecylenic acid appear at 3078 cm^{-1} and 1643 cm^{-1} and the peaks of epoxy groups at 910 cm^{-1} disappear in the spectra of UROP, indicating the competence of ring-opening reaction of epoxidized rapeseed oil and the successfully graft of 10-undecylenic acid. The absorption peaks of carbonyl groups of UROO are composed of two peaks: the peaks at 1743 cm^{-1} are associated with the carbonyl of the rapeseed oil triglycerides, and the other peaks at 1733 cm^{-1} belong to the characteristic absorption of the newly formed ester. The peaks at 3078 cm^{-1} and 1643 cm^{-1} of UROO ascribes to the terminated double bonds of 10-undecylenic acid. The enhancement of these peaks shows that more terminated double bonds have been grafted in UROO. The NMR and FTIR results demonstrate that the UROO was successful prepared by these two steps.

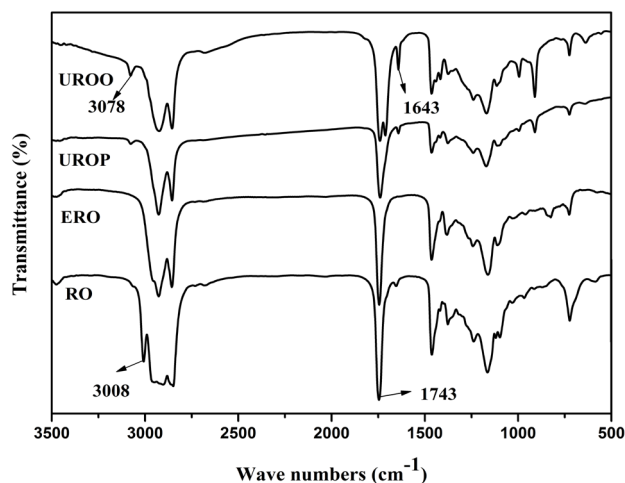


Figure 3: FTIR spectra of RO, ERO, UROP and UROO

3.2 Cure Kinetics of Thiol-ene Reaction Between UROO and Thiol

The cure kinetics of thiol-ene reaction between UROO and PETMP with formulation CF3 were monitored by FTIR. Before curing, the double bonds ($=\text{CH}_2$ stretch, 3078 cm^{-1}) and thiol (S-H stretch, 2570 cm^{-1}) peaks were obviously demonstrated in the FTIR spectra [31]. The evolution of the height of these two characteristic peaks is shown in Fig. 4. With the increase of the curing time, the intensity of both two peaks gradually decreases, indicating the occurrence of the polymerization of UROO and thiol under the irradiation of UV. Fig. 5 shows instantaneous conversions (calculated from FTIR spectra) of the ene and thiol functional groups. The conversion of these two functional groups increase with curing time and the conversion of carbon-carbon double bonds is higher than thiol conversion. From the Fig. 5, it was found that the conversion of the terminal double bonds and thiol groups at 30 minutes were around 79 and 72%, respectively. This result is in agreement with previous report [23].

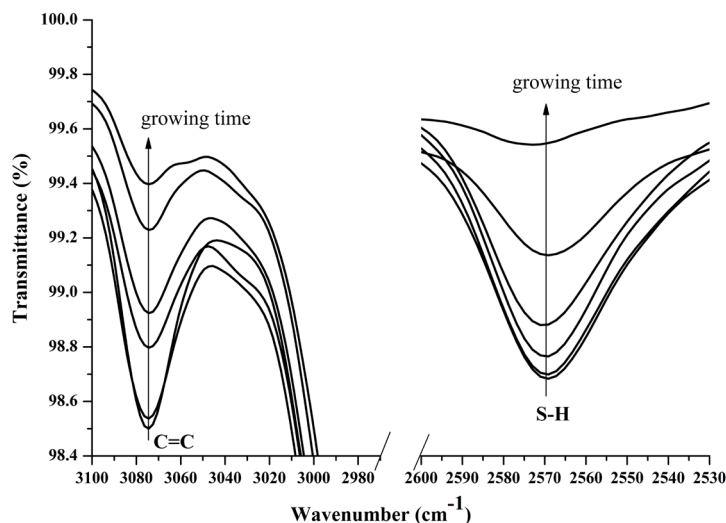


Figure 4: Decrease in the stretching vibration bands of the double bond at 3078 cm^{-1} and thiol functioning group at 2570 cm^{-1} of the CF3 formulation. The time interval between each spectrum is 2 minutes

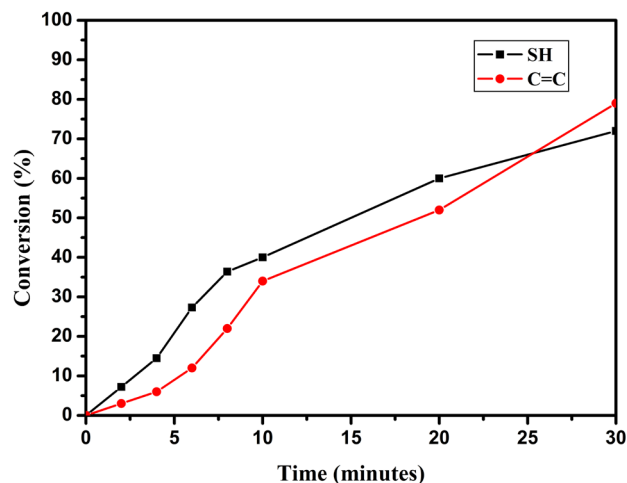


Figure 5: Conversion of double bond and thiol in the interval of 30 minutes

3.4 Characterization of the UV cured Films

After UV curing, the crosslinked polymers were formed via thiol-ene coupling of these polyfunctional vinyl oligomer and thiol monomers. The gel content is proportional to the crosslinking density and can be used as a parameter to indicate the efficiency of curing. In order to study the crosslinking density of the three UV cured bio-based films, the gel content was obtained through dichloromethane extraction. The gel contents of CF1, CF2 and CF3 were 69.77%, 88.53% and 93.65%, respectively (as shown in Tab. 2). These gel content values indicate that the UV curing system was highly, but not completely UV cured. Clearly, the CF3 exhibited the highest gel content, because PETMP has a higher functionality than other two thiol reagents. Higher cross-link density networks in films can be attributed to higher functionality [26]. The pendulum hardness data of UV cured films also confirms this conclusion. The hardness of the UV cured films increases with the increase of functionality of the thiol reagents. CF1 film shows the lowest hardness while CF3 has the highest hardness due to the difference of crosslink density [32].

Table 2: Gel content and pendulum hardness of the UV cured films

Sample code	CF1	CF2	CF3
Gel content (%)	69.77	88.53	93.65
Pendulum hardness (s)	4.2	5.6	6.0

The solvent swelling of the films can be used to study water resistance and hydrophobicity of the polymers, which is always influenced by the crosslink density of the film. All the polymers show the similar absorption behavior. With the increase of immersion time, the polymers first demonstrate a rapid absorption in the beginning stage. Then the absorption rate gradually decreases. After a certain immersion time, the absorption reaches a saturation stage. Among them, the polymer with the recipe of CF1 show the highest water-absorption rate while the polymer with the recipe of CF3 show the lowest water absorption rate as shown in Fig. 6. In addition, the water absorption of CF1 polymer reaches 21% after 168 h immersion while the water absorption of CF3 polymer is only 2% in the same immersion condition. Because high crosslinking density of CF3 polymer in inhibit the penetration of water into the films [33]. In contrast to water absorption, toluene uptake is much faster than that of water uptake and arrives at equilibrium condition within 72 h, due to the majority of solvent-soluble C15 long chain segments in UV cured films. Meanwhile, the toluene absorption also shows positive correlation with crosslink density of UV cured films. However, there is no big difference in the toluene-absorption rate for different polymers.

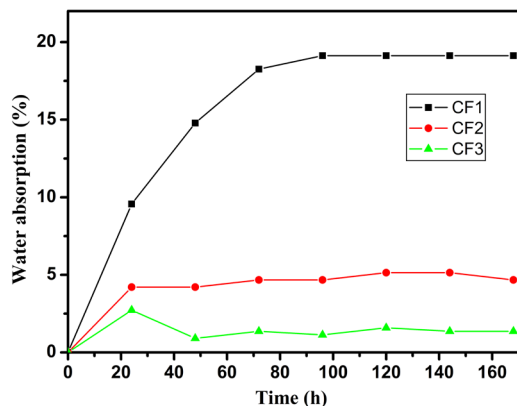


Figure 6: Water absorption-time diagram of the UV cured films

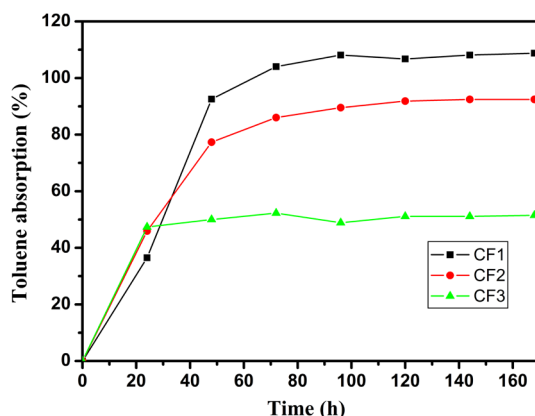


Figure 7: Toluene absorption-time diagram of the UV cured films

The thermal stability of thiol-ene UV-curable films was investigated by TGA and its derivative (DTG) in nitrogen atmosphere (Fig. 8). It can be seen that the four curves are similar. The onset temperature of decomposition was about 290°C. In the temperature ranging from 290 to 410°C, about 70% weight loss was observed, accompanying with an exothermic peak due to the decomposition of cross-linked terminal groups. An obvious exothermic peak occurred between 410 and 500°C, which accounts of 30% weight loss of the samples. This exothermic peak is attributed to the decomposition of the polymeric backbone. There is no obvious difference about TGA curve of these films, indicated that the degree of crosslinking almost demonstrates no effect on the thermal stability in this stage. It could be referred to the similar chemical structure of cross-linked backbone and functionalities. According to the Fig. 8, it can be found that the UV cured films showed good thermal resistance.

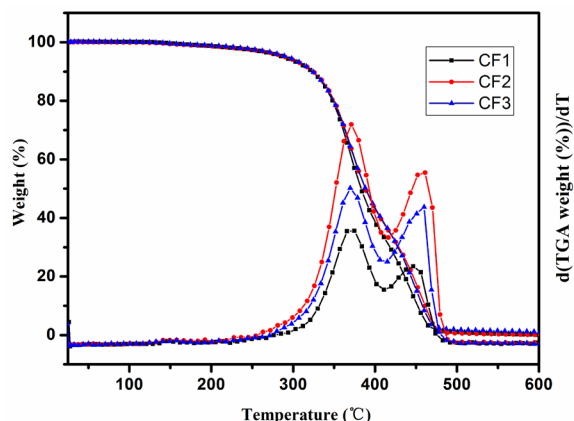


Figure 8: TGA and DTG of UV cured films

Fig. 9 shows storage modulus and loss factor as functions of temperature for UV cured films in the temperature range from -80 to 30°C . All polymers exhibit the similar trend for storage modulus as functions of temperature: At low temperature from -80°C , polymers are in the glassy state with storage moduli at the order of 400 - 1500 MPa, and then, storage moduli slightly decrease until a dramatic decline is observed. At high temperatures, the storage moduli of samples demonstrate a rubbery plateau. Meanwhile, all polymers only show one $\tan \delta$ peak, which was considered to be the glass transition temperature (T_g), indicating the homogeneous nature of all polymers. With the increase of functionality of the thiol monomer, the T_g of the resulting polymers increase. The polymers from PETMP show the highest T_g of 0°C while the polymers from has the lowest T_g of -22°C . Obviously, as the functionality of the thiol monomer increase, the storage moduli of the resulting polymers increase.

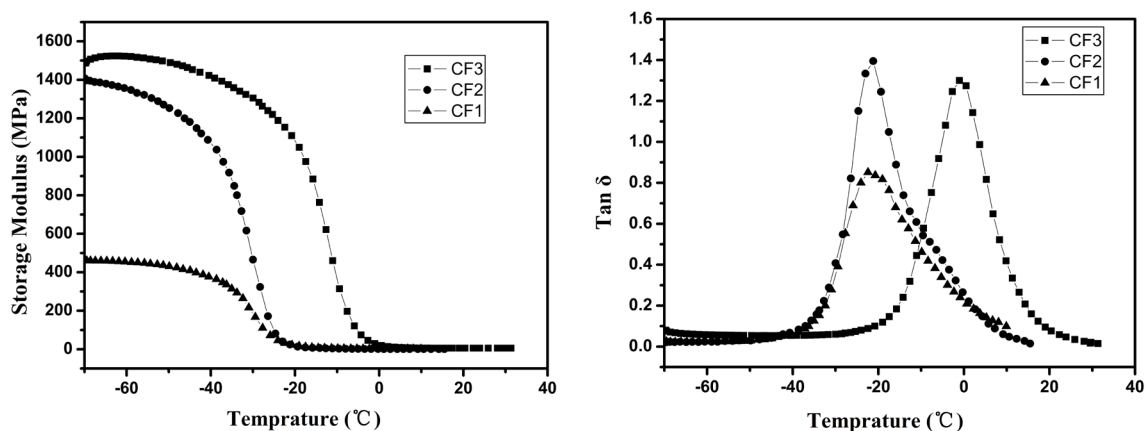


Figure 9: Storage moduli and loss factor ($\tan \delta$) as functions of temperature for UV cured films

4 Conclusion

A fully bio-based vinyl oligomer with high functionalities was successfully prepared by epoxidation of rapeseed oil, solvent-free and catalyst-free ring opening by 10-undecylenic acid, and esterification with 10-undecenoyl chloride. In addition, a series of renewable polymers were prepared by photo-polymerization of these modified vegetable oil and typical thiol monomers (pentaerythritol tetrakis (3-mercaptopropionate), pentaerythritol tris (3-mercaptopropionate) and 1,2-ethanedithiol. It is found that the polymers from 1,2-ethanedithiol exhibit the highest gel content, storage modulus and glass transition temperature due to the high crosslinking densities of the resulting polymers. All polymers show excellent

thermal stability up to 290°C. In addition, the resulting polymers exhibit good water resistance, which is promising to find application in green coatings and adhesives.

Notes: The authors declare no competing financial interest.

Acknowledgement: This work was sponsored by the National Natural Science Foundation of China (51563011), the Natural Science Foundation of Jiangxi Province (2016BAB203094), the Young Talents Project of Jiangxi Science and Technology Normal University (2016QNBjRC007) and the Postgraduate Innovation Fund Project of Jiangxi Science and Technology Normal University (YC2019-X31).

References

1. Goud, V. V., Pradhan, N. C., Patwardhan, A. V. (2006). Epoxidation of karanja (*Pongamia glabra*) oil by H₂O₂. *Journal of the American Oil Chemists Society*, 83, 635-640.
2. Xia, Y., Larock, R. C. (2010). Vegetable oil-based polymeric materials: synthesis, properties, and applications. *Green Chemistry*, 12, 1893-1909.
3. Milchert, E., Smagowicz, A., Lewandowski, G. (2010). Optimization of the epoxidation of rapeseed oil with peracetic acid. *Organic Process Research & Development*, 14, 1094-1101.
4. Liang, H. Y., Feng, Y., Lu, J. Y., Liu, L. X., Yang, Z. et al. (2018). Bio-based cationic waterborne polyurethanes dispersions prepared from different vegetable oils. *Industrial Crops and Products*, 122, 448-455.
5. Liu, Z., Erhan, S. Z., Akin, D. E., Barton, F. E. (2006). Green composites from renewable resources: preparation of epoxidized soybean oil and flax fiber composites. *Journal of Agricultural & Food Chemistry*, 54, 2134-2137.
6. Zhang, C., Garrison, T. F., Madbouly, S. A., Kessler, M. R. (2017). Recent advances in vegetable oil-based polymers and their composites. *Progress in Polymer Science*, 71, 91-143.
7. Liu, L. X., Lu, J. Y., Zhang, Y., Liang, H. Y., Liang, D. S. et al. (2019). Thermosetting polyurethanes prepared with the aid of a fully bio-based emulsifier with high bio-content, high solid content, and superior mechanical properties. *Green Chemistry*, 21, 526-537.
8. Espinosa, L. M. D., Meier, M. A. R. (2011). Plant oils: the perfect renewable resource for polymer science?!. *European Polymer Journal*, 47, 837-852.
9. Liang, H. Y., Wang, S. W., He, H., Wang, M. Q., Liu, L. X. et al. (2018). Aqueous anionic polyurethane dispersions from castor oil. *Industrial Crops and Products*, 122, 182-189.
10. Galià, M., Montero, D. E. L., Carles Ronda, J., Lligadas, G., Cádiz, V. et al. (2010). Vegetable oil-based thermosetting polymers. *European Journal of Lipid Science & Technology*, 112, 87-96.
11. Lu, Y., Larock, R. C. (2010). Novel polymeric materials from vegetable oils and vinyl monomers: preparation, properties, and applications. *Chemsuschem*, 2, 136-147.
12. Meier, M. A. R., Metzger, J. O., Schubert, U. S. (2007). Plant oil renewable resources as green alternatives in polymer science. *Chemical Society Reviews*, 36, 1788-1802.
13. Pelletier, H., Gandini, A. (2010). Preparation of acrylated and urethanated triacylglycerols. *European Journal of Lipid Science & Technology*, 108, 411-420.
14. Ronda, J. C., Lligadas, G., Galià, M., Cádiz, V. (2011). Vegetable oils as platform chemicals for polymer synthesis. *European Journal of Lipid Science & Technology*, 113, 46-58.
15. Liang, D., Zhang, Q., Zhang, W., Liu, L., Liang H. et al. (2019). Tunable thermo-physical performance of castor oil-based polyurethanes with tailored release of coated fertilizers. *Journal of Cleaner Production*, 210, 1207-1215.
16. Senyurt, A. F., Wei, H., Phillips, B., Cole, M., Nazarenko, S. et al. (2006). Physical and mechanical properties of photopolymerized thiol-ene/acrylates *Macromolecules*, 39, 6315-6317.

17. Shibata, M., Obara, S. (2012). Photo-cured organic-inorganic hybrid composites of acrylated castor oil and methacrylate-substituted polysilsesquioxane. *Journal of Applied Polymer Science*, 126, 1-9.
18. Chan, J. W., Shin, J., Hoyle, C. E., Bowman, C. N., Lowe, A. B. (2010). Synthesis, thiol-yne "click" photopolymerization, and physical properties of networks derived from novel multifunctional alkynes. *Macromolecules*, 43, 4937-4942.
19. Zhang, C., Yan, M., Cochran, E. W., Kessler, M. R. (2015). Biorenewable polymers based on acrylated epoxidized soybean oil and methacrylated vanillin. *Materials Today Communications*, 5, 18-22.
20. Chen, G., Kumar, J., Gregory, A., Stenzel, M. H. (2009). Efficient synthesis of dendrimers via a thiol-yne and esterification process and their potential application in the delivery of platinum anti-cancer drugs. *Chemical Communications*, 12, 6291-6293.
21. Zhang, P., Zhang, J. W. (2013). One-step acrylation of soybean oil (SO) for the preparation of SO-based macromonomers. *Green Chemistry*, 15, 641-645.
22. Chiou, B. S., Khan, S. A. (1997). Real-time FTIR and in Situ rheological studies on the UV curing Kinetics of thiol-ene polymers. *Macromolecules*, 30, 7322-7328.
23. Black, M., Rawlins, J. W. (2009). Thiol-ene UV-curable coatings using vegetable oil macromonomers. *European Polymer Journal*, 45, 1433-1441.
24. Hensarling, R. M., Doughty, V. A., Chan, J. W., Patton, D. L. (2009). "Clicking" polymer brushes with thiol-yne chemistry: indoors and out. *Journal of the American Chemical Society*, 131, 14673-14675.
25. Konkolewicz, D., Gray-Weale, A., Perrier, S. (2009). Hyperbranched polymers by thiol-yne chemistry: from small molecules to functional polymers. *Journal of the American Chemical Society*, 131, 18075-18077.
26. McNair, O. D., Sparks, B. J., Janisse, A. P., Brent, D. P., Patton, D. L. et al. (2013). Highly tunable thiol-ene networks via dual thiol addition. *Macromolecules*, 46, 5614-5621.
27. Dillman, B. F., Na, Y. K., Jessop, J. L. P. (2013). Solventless synthesis and free-radical photopolymerization of a castor oil-based acrylate oligomer. *Polymer*, 54, 1768-1774.
28. Senyurt, A. F., Wei, H., Hoyle, C. E., Piland, S. G., Gould, T. E. (2007). Ternary thiol-ene/acrylate photopolymers: effect of acrylate structure on mechanical properties. *Macromolecules*, 40, 4901-4909.
29. Feng, Y., Liang, H., Yang, Z., Yuan, T., Luo, Y. et al. (2017). A solvent-free and scalable method to prepare soybean oil-based polyols by thiol-ene photo-click reaction and biobased polyurethanes therefrom. *ACS Sustainable Chemistry & Engineering*, 5 (8), 7365-7373.
30. Fu, C. Q., Liu, J. C., Xia, H. Y., Shen, L. (2015). Effect of structure on the properties of polyurethanes based on aromatic cardanol-based polyols prepared by thiol-ene coupling. *Progress in Organic Coatings*, 83, 19-25.
31. Petrovic, Z. S. (2008). Polyurethanes from vegetable oils. *Polymer Reviews*, 48, 109-155.
32. Zhang, C. Q., Xia, Y., Chen, R., Huh, S., Johnston, P. A. et al. (2013). Soy-castor oil-based polyols prepared using a solvent-free and catalyst-free method and polyurethanes therefrom. *Green Chemistry*, 15, 1477-1484.
33. Zovi, O., Lecamp, L., Loutelierbourhis, C., Lange, C. M., Bunel, C. (2011). A solventless synthesis process of new UV-curable materials based on linseed oil. *Green Chemistry*, 13, 1014-1022.